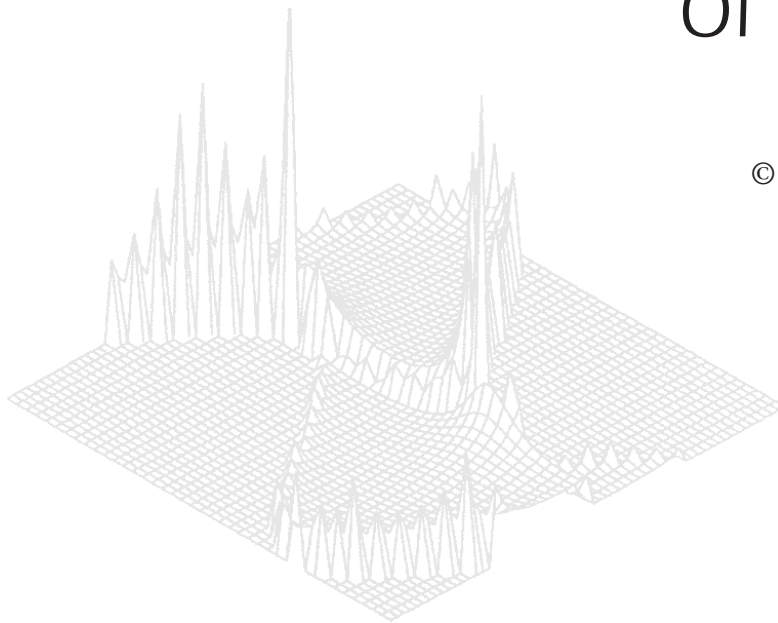

C S I R O P U B L I S H I N G

Australian Journal of Physics

Volume 52, 1999
© CSIRO Australia 1999



A journal for the publication of
original research in all branches of physics

www.publish.csiro.au/journals/ajp

All enquiries and manuscripts should be directed to

Australian Journal of Physics

CSIRO PUBLISHING

PO Box 1139 (150 Oxford St)

Collingwood

Vic. 3066

Australia

Telephone: 61 3 9662 7626

Facsimile: 61 3 9662 7611

Email: peter.robertson@publish.csiro.au



Published by **CSIRO PUBLISHING**
for CSIRO Australia and
the Australian Academy of Science



Magnetic Stress in Solar System Plasmas*

C. T. Russell

Department of Earth and Space Sciences, Institute of Geophysics and Space Physics,
University of California, Los Angeles, CA 90095–1567, USA.

Abstract

Magnetic stresses play an important role in the dynamics of geophysical systems, from deep inside the Earth to the tenuous plasmas of deep space. In the magnetic dynamos inside the sun and the planets, the magnetic stresses of necessity rival the interior mechanical stresses. In solar system plasmas, magnetic stresses play critical roles in the transfer of mass, momentum and energy from one region to another. Coronal mass ejections are rapidly expelled from the sun and their interplanetary manifestations plough through the pre-existing solar wind. Some of these structures resemble flux ropes, bundles of magnetic field wrapped around a central core, and some of these appear to be almost force-free. These structures and similar ones in planetary magnetospheres appear to be created by the mechanism of magnetic reconnection. Solar system plasmas generally organise themselves in giant cells in which the properties are rather uniform, separated by thin current layers across which the properties change rapidly. When the magnetic field on the two sides of one of these current layers changes direction significantly (by over 90°), the magnetic field on opposite sides of the boundary may become linked across the current sheet. If the resulting magnetic stress can accelerate the plasma out of the reconnection region, the process will continue uninterrupted. If not, the process will shut itself off. Such continuous reconnection can occur at the Earth's magnetopause and those of the magnetised planets. Reconnection in the terrestrial magnetotail current sheet and the jovian current sheet occurs in a setting in which the flow can be blocked on one side, causing reconnection to be inherently time-varying. At Jupiter, this mechanism also separates heavy ions from magnetospheric flux tubes so that the ions can escape but Jupiter can retain its magnetic field. Despite the very wide range of parameters and scales encountered in heliospheric plasmas, there is surprising coherence in the mechanisms in these varying environments.

1. Introduction

Magnetic fields pervade the universe. Sometimes these fields are very weak. In interstellar space, they are perhaps a million times weaker than on the surface of the Earth. In contrast, the magnetic fields of stars can be many orders of magnitude greater than the terrestrial field. At both extremes, however, the magnetic field is dynamically important to the environment in which these fields are found. In a non-electrically-conducting environment the situation is quite

* Refereed paper based on a plenary lecture presented on 30 September 1998 to the 13th AIP National Congress held in Fremantle, Western Australia.

different. For example, on the surface of the Earth, where the gases are neutral and not electrically conducting, we tend to consider the magnetic field as once useful for navigation but now mainly a curiosity. We underestimate its importance to our increasingly technological society, which depends on the Earth's giant magnetic shield.

Deep inside the Earth and high in the atmosphere the magnetic field assumes much greater importance. The fluid motions in the electrically conducting core of the Earth generate magnetic fields that react back on those motions. The magnetic field generated in the core extends far into space, where it interacts with the magnetic field and plasma from the sun. The magnetic field shields the Earth from the full onslaught of energetic charged particles from the sun, but also takes some fraction of these particles and accelerates them to high energies into the atmosphere, causing the aurora. The aurora was in fact probably the first phenomenon observed by man that was caused by magnetic processes, well before the discovery of the terrestrial magnetic field as an aid to navigation or that of sunspots, the dark areas in the photosphere caused by strong magnetic fields. Here we examine some of the magnetic phenomena observed in solar system plasmas, looking at both static magnetic structures and dynamical processes. The scale sizes of structures and the plasma conditions vary widely across these various phenomena. Nevertheless we find much similarity in the behaviour of these diverse systems.

Before examining these structures and processes, we first examine the equations that govern the underlying forces, and examine a few simple examples of how these equations are applied. The momentum equation for a typical space plasma is

$$\rho(\partial\mathbf{u}/\partial t + \mathbf{u}\nabla\mathbf{u}) = -\nabla p + \mathbf{j} \times \mathbf{B} + \rho F_g/m_p. \quad (1)$$

The magnetic force term $\mathbf{j} \times \mathbf{B}$ can be rewritten as

$$((\nabla \times \mathbf{B}) \times \mathbf{B})/\mu_0 = -\nabla B^2/2\mu_0 + (\mathbf{B} \cdot \nabla)\mathbf{B}/\mu_0. \quad (2)$$

The term $B^2/2\mu_0$ is the magnetic pressure, and its gradient is a force like that of the gradient of the thermal pressure of the plasma. The term $(\mathbf{B} \cdot \nabla)\mathbf{B}/\mu_0$ can be decomposed into two components. The first, $\hat{\mathbf{b}}\hat{\mathbf{b}} \cdot \nabla B^2/2\mu_0$, where $\hat{\mathbf{b}}$ is a field-aligned unit vector, cancels the field-aligned part of the pressure gradient. Thus magnetic pressure acts only perpendicular to the magnetic field lines. The second component is $(B^2/\mu_0)\hat{\mathbf{b}} \cdot \nabla\hat{\mathbf{b}}$, or $-\mathbf{n}B^2/\mu_0 R_c$, where R_c is the radius of curvature. This is the curvature force, sometimes called magnetic tension. Now let us apply the equation for magnetic force to a dipole magnetic field, field lines of which are sketched in Fig. 1. There is no plasma here, nor any currents flowing except in a small volume at the centre of the dipole field. Thus the $\mathbf{j} \times \mathbf{B}$ force is zero outside the geodynamo region. The two components of this force, the outward magnetic pressure force associated with the radially decreasing magnetic field strength and the inward force due to the curvature of the magnetic field, exactly balance everywhere.

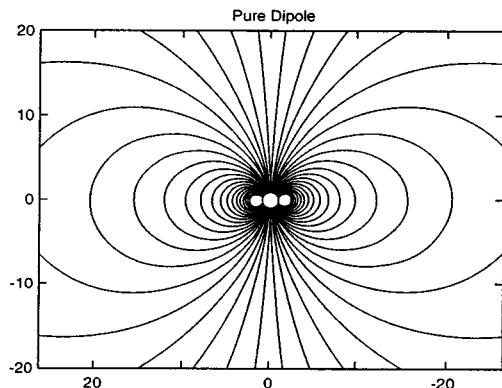


Fig. 1. Magnetic field lines of a dipole in a vacuum. The inward magnetic curvature force balances the outward magnetic pressure gradient force in this current-free situation.

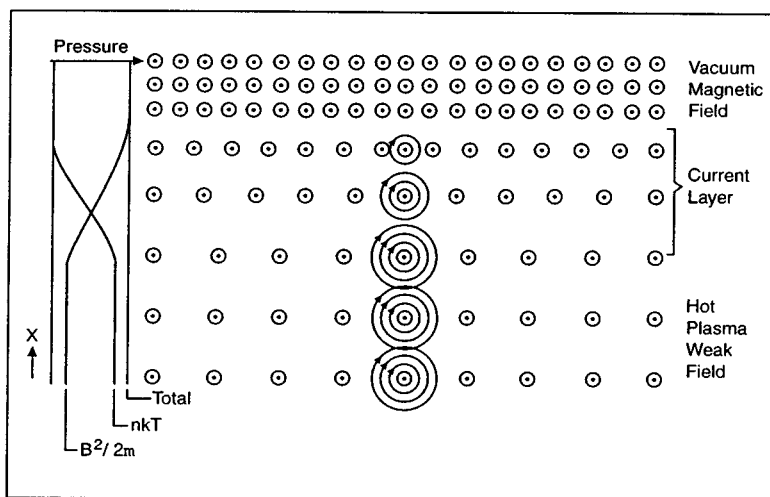


Fig. 2. Pressure balance between a hot magnetised plasma and a vacuum magnetic field. The pressure gradient force acts in the upward direction; the magnetic pressure gradient force acts in the downward direction. Here a current flows that creates a $\mathbf{j} \times \mathbf{B}$ force on the plasma.

In the vacuum dipole field we balanced magnetic forces against each other but in a typical magnetised plasma in the solar system there are forces due to the thermal pressure gradients, gravitational and centrifugal forces. To illustrate the static pressure balance in a magnetised plasma, we examine in Fig. 2 a situation in which there is a vacuum magnetic field out of the page at the top and a hot plasma with a weaker magnetic field in the same direction at the bottom of the figure, with a region of transition between them in which the field weakens and the plasma energy density increases (downward). The orbits of some of the ions in this plasma are sketched. Electrons orbit the field in the reverse direction but since they carry negative charge, they cause currents about the field in the same direction as the ions.

We can divide Fig. 2 into three parts: the vacuum homogeneous region, in which there is no current; the hot plasma region, in which currents circulate around the field lines (and hence reduce the field strength via diamagnetism) but in which there is no net current in any direction; and a transition region, in which there is a net current as signified by the gradient in the magnetic field. In this region there is a $\mathbf{j} \times \mathbf{B}$ force applied to the plasma; here it is totally due to the magnetic pressure gradient term. It is balanced by the pressure gradient force in the plasma pushing upward. In solar system plasmas this simple pressure balance between a region of strong magnetic field and a hot static plasma is a very common situation.

Before proceeding to our examination of solar system plasmas, we should also mention how magnetic fields are generated by stars and planets. To visualise this process we need only three equations: Ampere's law, Ohm's law and Faraday's law. In our moving magnetised plasma there is an electric field contribution due to the motion of the conducting fluid that must be included in Ohm's law. Our three equations are:

$$\text{Ampere's law} \quad \nabla \times \mathbf{B} = \mu_0(\mathbf{j} + \epsilon_0 \partial \mathbf{E} / \partial t), \quad (3)$$

$$\text{Ohm's law} \quad \mathbf{j} = \sigma(\mathbf{E} + \mathbf{u} \times \mathbf{B}), \quad (4)$$

$$\text{Faraday's law} \quad \partial \mathbf{B} / \partial t = -\nabla \times \mathbf{E}. \quad (5)$$

In space plasmas we can generally ignore the displacement current. Taking the curl of (2) and substituting (1) and (3), we obtain the induction or dynamo equation

$$\partial \mathbf{B} / \partial t = \nabla \times (\mathbf{u} \times \mathbf{B}) + \nabla^2 \mathbf{B} / \mu_0 \sigma. \quad (6)$$

This equation shows that the convective terms compete with dissipation in a magnetised plasma to maintain or alter the magnetic field. The ratio of the two terms on the right-hand side is the magnetic Reynolds number. This number is usually $\gg 10^6$ in space plasmas for large-scale processes. Thus for all practical purposes we may consider the plasma to be frozen to the magnetic field in treating these systems.

The dynamo equation demonstrates that in a dynamo region the changing magnetic field is a combination of convective effects competing with dissipation effects, but it does not show us precisely what those fluid motions are that produce the observed field. This work is still on going but numerical simulations with computers now can produce credible self-reversing dynamos from the basic equations of magnetohydrodynamics. We can intuitively see how a dynamo might work by examining Fig. 3, which shows three separate steps of what has been called the alpha-omega dynamo (Parker 1979). The omega refers to the differential rotation needed to twist up the field. The alpha refers to the second twist introduced by Coriolis forces on rising convection cells. In Fig. 3*a* we have an undisturbed dipole-like field confined to meridians of a rotating body. This is called the poloidal field. The body rotates at a different rate at different depths twisting the poloidal field as shown in Fig. 3*b*. This out-of-plane component is

called the toroidal field. Finally, convection lifts the toroidal field vertically and Coriolis forces cause the cell of rising magnetised fluid to twist, creating poloidal field from the toroidal field and thus completing the cycle by regenerating the original poloidal field. The actual details of the behaviour of magnetic dynamos are quite complex but the basic elements are thought to be included in this very simple exposition.

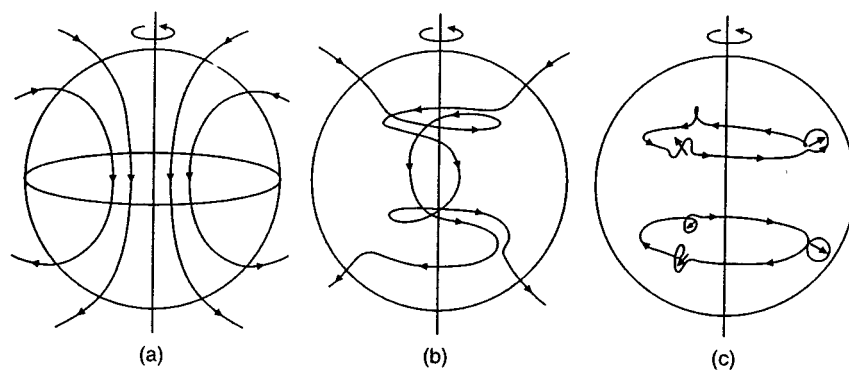


Fig. 3. Three stages of the regeneration of the magnetic field of the alpha-omega dynamo. The poloidal magnetic field in the left-hand panel is twisted by the differential rotation of the body to form a toroidal component in the middle panel. Vertical convection lifts the toroidal field and Coriolis forces twist the field, creating poloidal field in the right-hand panel, thus recreating the original field. [After Russell (1986).]

In the solar system the scales can be, well, astronomical but the pressures and magnetic field strengths are very small, of the order of nanopascals and nanoteslas respectively. The solar wind is supersonic so that the ions' bulk velocity is much greater than the ion thermal speed. Thus the main pressure that the solar wind exerts on the planets is due to what we call dynamic pressure, the solar wind momentum flux. Nevertheless because a supersonic flow cannot be deflected around a planet without the formation of a shock, this dynamic pressure is converted to thermal and magnetic pressure by the time the obstacle is reached. There are basically two types of obstacles to the solar wind flow: the planetary atmosphere and the planetary magnetosphere. Fig. 4 illustrates the interaction of the former type of obstacle with the solar wind (see for example Luhmann 1995). Solar extreme ultraviolet radiation ionises the upper atmosphere of a planet and the thermal pressure exceeds the dynamic pressure of the solar wind so that it is deflected at high altitudes. As mentioned above, the supersonic nature of the solar wind necessitates the formation of a bow shock to deflect the flow. This bow shock stands off at a distance that allows the compressed flow to pass between the shock and the obstacle. An important aspect of the interaction, not illustrated here, is that the bulk flow is very slow as the obstacle is approached but the thermal velocity remains high. Thus the ions can move away from the subsolar region along the field lines, effectively evacuating this region and leaving an interface similar to that sketched in Fig. 2, with the strong magnetic field in the magnetosheath and the high plasma pressure on the planetary side of the boundary.

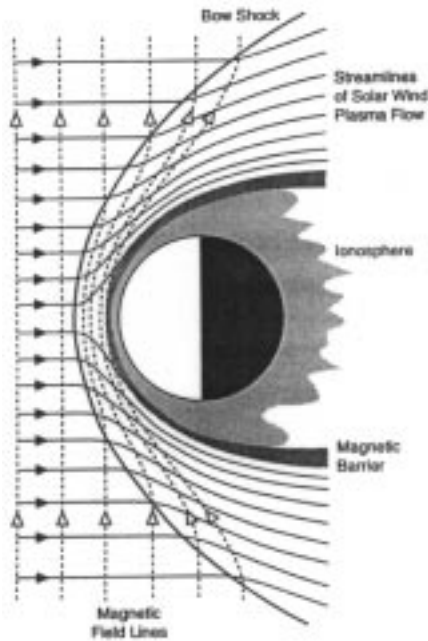


Fig. 4. Solar wind interaction with an unmagnetised planet. The extreme ultraviolet radiation from the Sun ionises the atmosphere of the planet. This ionosphere has greater pressure than that of the solar wind flow so that the solar wind is deflected. Since the solar wind is supersonic, a shock front is formed in order to deflect the flow. Close to the obstacle on the upstream side the plasma moves along the field leaving a near-vacuum magnetic barrier to transmit the pressure to the ionosphere.

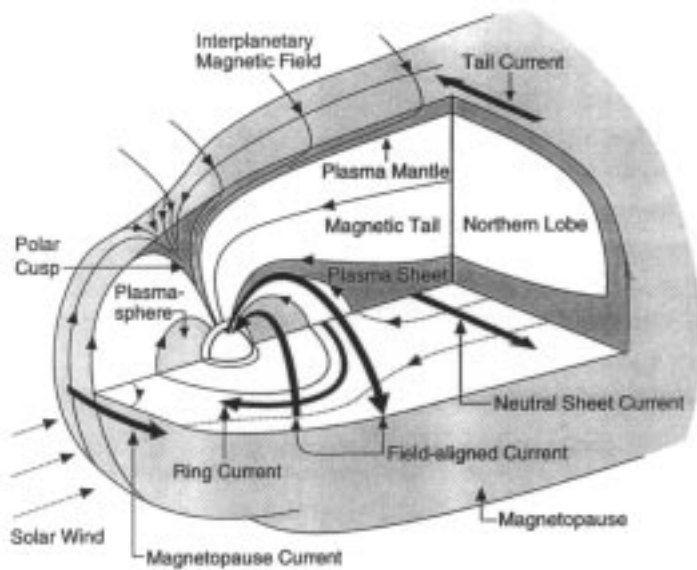
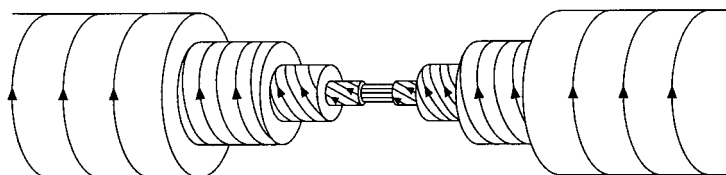


Fig. 5. Three-dimensional cutaway sketch of the Earth's magnetosphere, showing the principal currents and flows as well as the magnetic and plasma configuration. [After Russell (1995).]

If the planetary magnetic field is strong, then the second type of obstacle is formed. The solar wind is deflected far above the planetary atmosphere and an interaction like that shown in Fig. 5 occurs (see e.g. Walker and Russell 1995). As before there is a standing bow shock (not shown) but now there is a strong

magnetic obstacle between the shocked solar wind plasma (the magnetosheath) and the planet. The interface between the plasma and the magnetic field of the obstacle is called the magnetopause. The fact that there are magnetic fields on either side of the magnetopause allows very interesting interactions to occur for varying directions of the interplanetary field. Important in this interaction is the magnetic tail region on the antisolar side of the Earth, which can act as a reservoir of stored energy for powering auroral processes.



Interior Structure of Flux Rope

Fig. 6. Structure of a magnetic flux rope. In the interior the magnetic field is strong and axial. The magnetic pressure gradient force pushes outward, balanced by the curvature force of the twisted field around the axis. Currents flow to maintain the twist. If the current flows solely along the magnetic field, the structure is termed force-free. [After Russell and Elphic (1979).]

The final magnetic structure that requires some introduction is the magnetic flux rope shown in Fig. 6 (see for example Priest 1995). In the flux rope shown, the magnetic field is strong in the centre and weakens with radial distance from the centre of the rope. Thus there is a magnetic pressure force outward. There is also an increasing twist in the rope with radial distance. The curvature force of this azimuthal component counteracts the magnetic pressure force. If plasma pressure plays no role in this process and the structure is in equilibrium, it is called a force-free flux rope. Currents are indeed flowing in such a structure, as they are needed to decrease the field strength and to twist it, but the plasma pressure remains the same throughout the rope. Such structures are surprisingly prevalent in the solar system, from the solar corona to the ionosphere of Venus to the magnetotail of the Earth.

2. Interplanetary Coronal Mass Ejections

During a solar eclipse we can see with the naked eye the light scattered from the electrons in the solar corona. These images reveal a very structured coronal density controlled by the sun's magnetic field, but they provide only a snapshot of the density structure and reveal nothing about its dynamics. It was not until the coronagraph measurements on the *SkyLab* mission, in which the light from the sun's photosphere was permanently blocked with an occulting disk, that pictures of the dynamical changes of the electron density could be made. These images revealed the rather frequent production of expanding loops or bubbles of high-density plasma, called coronal mass ejections, that could be followed for about 4 hours, out to about 4 solar radii (e.g. Hundhausen 1995).

Spacecraft in the inner heliosphere in turn found evidence for the interplanetary manifestations of these structures, which have been called interplanetary coronal

mass ejections, ICMEs. Magnetic and solar wind measurements of such structures are shown in Figs 7a and 7b. Large magnetic fields that slowly rotate and cold ions manifest these structures. Often the magnetic structure can be modelled by a magnetic rope, and sometimes these ropes appear to be nearly force-free, as shown in Fig. 6. At times the ropes show evidence for expansion. They drive shocks on their leading edges and have magnetic profiles whose field magnitudes decrease with time, as illustrated in Fig. 7a. The cold ion temperatures in all ropes indicate that at one time the rope expanded rapidly in a region of low heat flux.

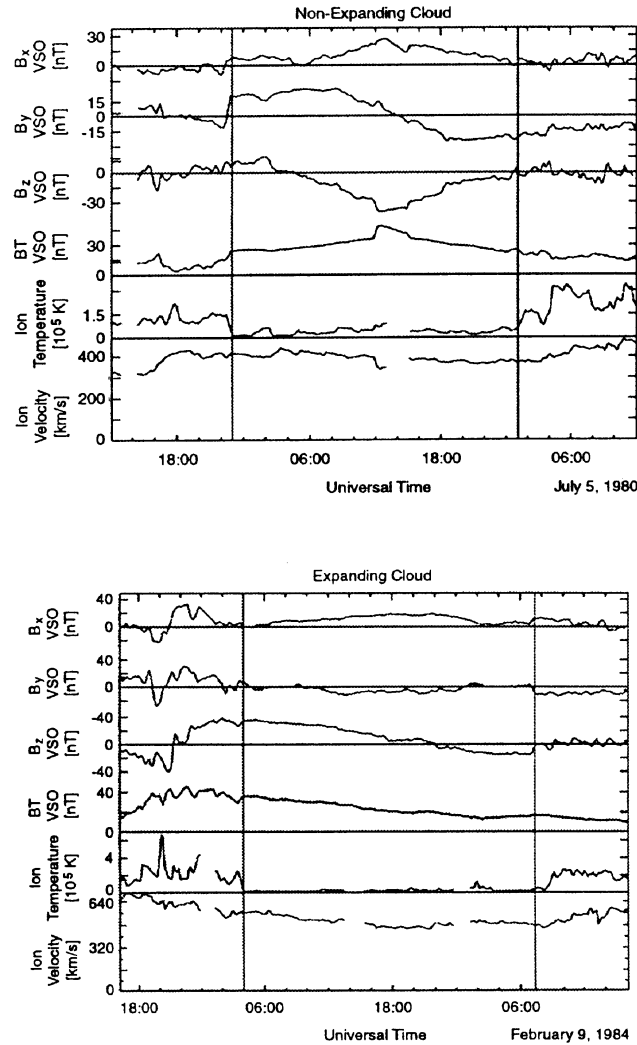


Fig. 7. Examples of interplanetary coronal mass ejections. The top four panels show the magnetic field in Venus solar orbital coordinates with B_x toward the sun, B_y opposite planetary motion and B_z northward along the Venus orbital pole. The bottom panels show the ion temperature and bulk velocity. The left-hand panel shows an ICME that appears to have stopped expanding, having assumed an almost force-free profile. The right-hand panel shows an example of an ICME that appears to be still expanding, resulting in a decreasing magnetic field magnitude with time.

Fig. 8 shows the existing paradigm for such magnetic clouds, as they have been called. The true picture is probably much more complicated than this, with multiple ropes being produced in any one coronal mass ejection. The leading polarity is controlled by the overall global magnetic field of the sun, and their average orientation changes in the course of the solar cycle. These structures are very important for us on Earth because they produce the greatest levels of geomagnetic disturbance. These disturbances can affect radio communications by disrupting the ionosphere, cause failures in operating spacecraft through various energetic particle effects, and cause power blackouts through the overloading of long, high-voltage transmission lines.

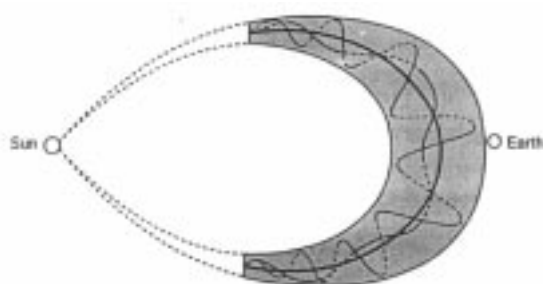


Fig. 8. Current paradigm of a force-free ICME. The top panel shows the flux rope connecting outward from the sun. [After Lepping *et al.* (1990).]

Fig. 9 illustrates how these rope-like structures might be made by magnetic reconnection in the solar corona. Stretched-out loops create oppositely directed regions of magnetic field that join up and change partners, altering the topology of the field. Multiple reconnections lead to detached structures. As they pass the Earth these structures can be 50 million km across. To find magnetic structures with sizes at the other end of the scale we next visit Venus.

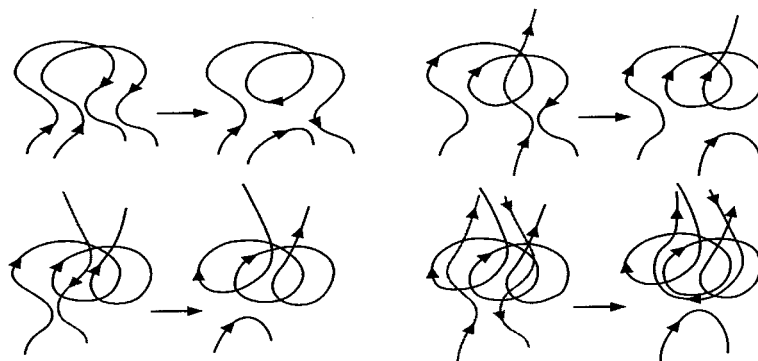


Fig. 9. Mechanism for generating a detached ICME flux rope through reconnection of coronal magnetic fields.

3. Interaction of Flowing Magnetised Plasma with a Neutral Gas

When a flowing magnetised plasma encounters a neutral gas, it generally picks up some of that gas in the form of ions. This ionisation may be produced

by ordinary collisions, by charge exchange or by photoionisation. In a dense atmosphere in the presence of a strong extreme ultraviolet source, such as the sun, sufficient ions may be produced to exclude the flow from some portion of the volume around the body producing the neutral atmosphere. This happens in the interaction of the solar wind with Venus, Mars and some of the larger comets. Fig. 10 illustrates the magnetic geometry of the solar wind interaction with Venus, perhaps the best studied of this class of interactions. The principal difference between the interaction of the solar wind with Venus and with a comet is that Venus' gravitational field confines the atmosphere to a limited region about 15 000 km across, whereas the atmosphere of a comet, though much more rarefied, extends to over a million km. As a result the number of ions added to the flow in such an interaction is much greater at a comet, whose nucleus may only be about 10 km across, than at a much bigger planet.

Fig. 10 shows three magnetic field lines at seven times during their passage by Venus, a planet with no intrinsic magnetic field. The lowest of the three field lines approaches most closely to Venus. It picks up the most new ions and it slows down more at its closest approach to the planet than the other two field lines. The field lines are straight beyond the bow shock and are totally unaffected by the interaction. Behind Venus the three field lines become stretched out. The curvature force and the magnetic pressure force both act to accelerate the plasma down the tail. This acceleration eventually allows the magnetic field lines to straighten up, and the only signature of the interaction far downstream is the presence of planetary ions, generally singly ionised oxygen. The Venus magnetotail has been statistically mapped and the magnetic forces calculated (McComas *et al.* 1986). Fig. 11 shows the current, the forces and the velocity deduced from these maps. The forces act to confine the plasma to the centre of the tail and to accelerate it such that by about 12 Venus radii downstream, the velocity of the plasma reaches the velocity of the upstream solar wind. This same process accelerates plasma in comet tails and at the moon Io in the jovian magnetosphere.

Now let us change scale sizes and plasma conditions and enter the ionosphere of Venus itself, the region where we should expect zero magnetic field strength. Fig. 12 shows the electron number density and the magnetic field strength as a function of altitude on a typical pass through the Venus ionosphere by the *Pioneer* Venus orbiter (Russell 1990). The region of strong magnetic field at the top is the magnetic barrier region in pressure balance with the ionospheric plasma in the lower two-thirds of the figure. What is of interest to us here are the very narrow enhancements in the field strength in the lower part of the figure. These enhancements are very tiny flux ropes, as small as 1 km across. We believe that these ropes are pulled down into the ionosphere by the curvature force of the field lines draped over the spherical ionosphere. Using a simple model of a magnetic rope, but one that is not necessarily force-free, we can model the variation in the magnetic field as shown in Fig. 13, which shows hodograms of the field variation, plots of one component of the field versus another (Elphic and Russell 1983). Fig. 14 shows the magnetic field strength and the angle of the magnetic field to the axis of the rope, together with the calculated parallel and perpendicular currents. For this particular rope the current is principally along the rope axis so that it is nearly force-free.

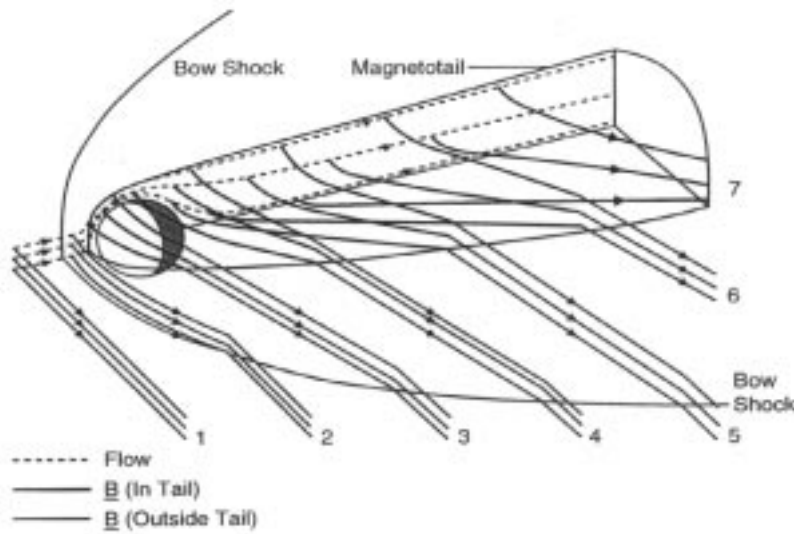


Fig. 10. Schematic illustration of the formation of the magnetotail of an unmagnetized planet such as Venus or Mars. [After Saunders and Russell (1986).]

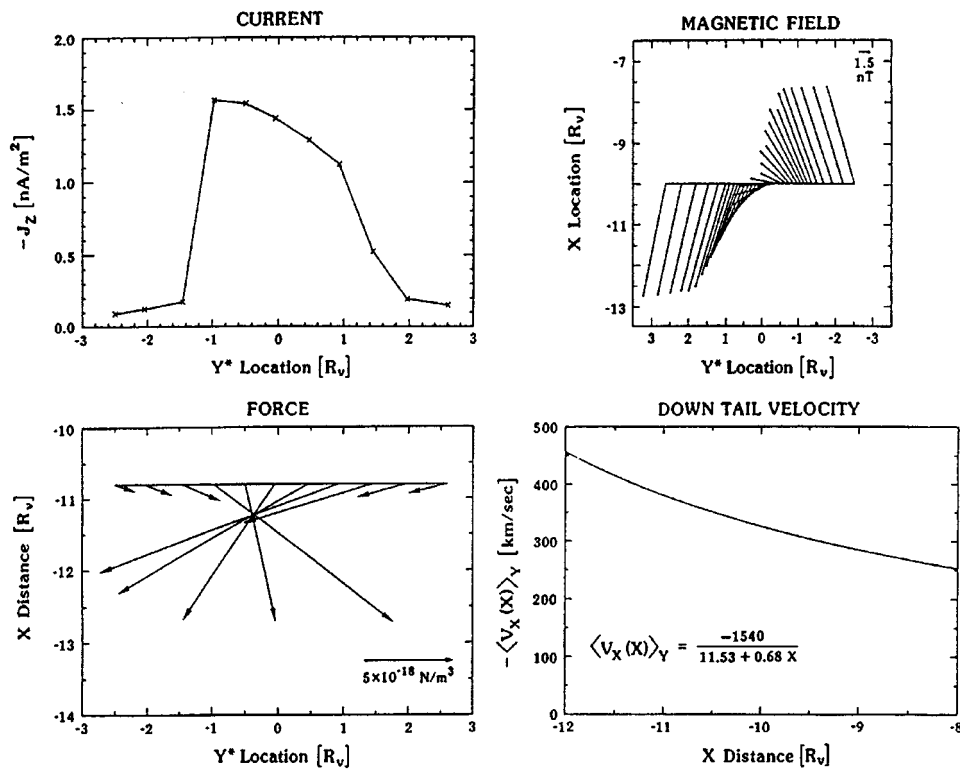


Fig. 11. Force balance in the Venus magnetotail (McComas *et al.* 1986). Upper right panel shows the average magnetic field configuration at $10R_V$ behind Venus. Upper left panel shows the electric current as a function of cross-tail position at this point. The lower left panel shows the $\mathbf{j} \times \mathbf{B}$ force on the tail plasma as a function of cross-tail position at $10R_V$ downtail. The lower right panel shows how this force accelerates the bulk velocity of the plasma with increasing down-tail distance.

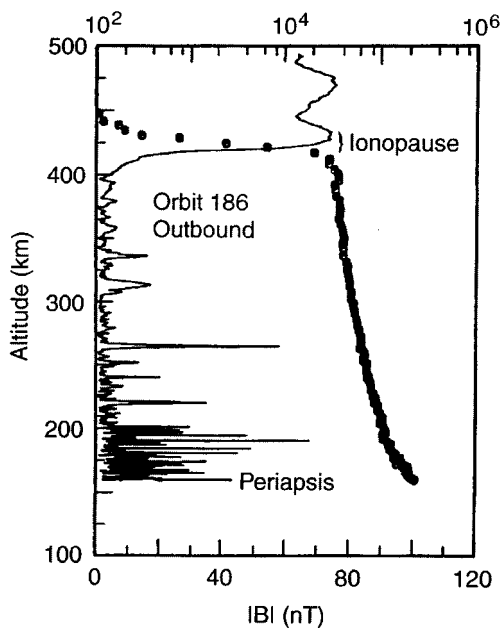


Fig. 12. Vertical profile of electron density (squares) and magnetic field strength (solid line) in the Venus ionosphere, illustrating the presence of thin magnetic filaments at low altitudes. The high-field region at the top of the panel is the magnetic barrier whose pressure is determined by the solar wind. The bottom of the ionosphere is at about 140 km. This altitude was not probed on this orbit. The top horizontal scale is the number density of electrons per cm³. [After Russell (1990).]

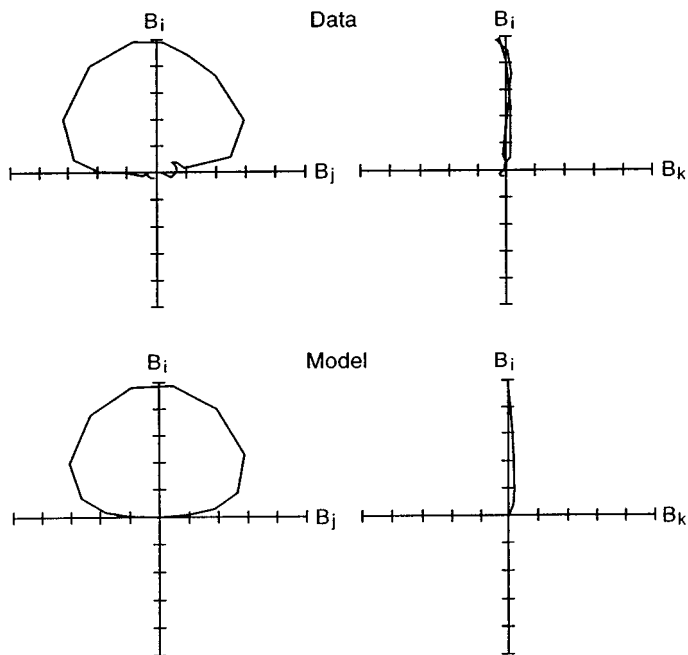


Fig. 13. Hodograms of the magnetic field observed during passage through a Venus flux rope (top) and through an analytical model (bottom). The two planes show orthogonal projections of the tip of the magnetic vector during the passage through the flux rope. In three-dimensional space the end of the magnetic vector traces a bent potato chip shape.

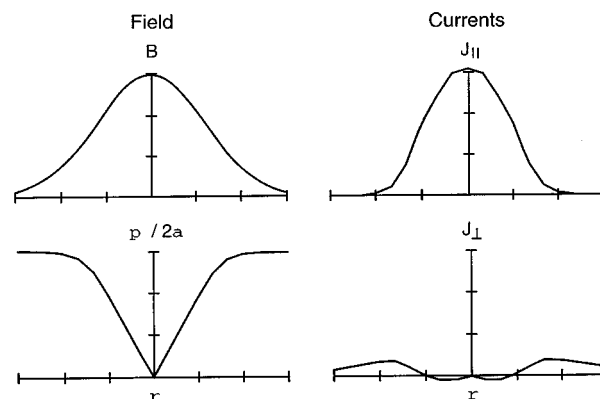


Fig. 14. Radial profiles through a model flux rope that has been fitted to a particularly force-free Venus flux rope. The upper left panel shows the magnetic field strength, lower left the angle of the magnetic field to the rope axis, upper right the parallel electric current, and lower right the perpendicular current.

The flux-rope nature of the ICMEs we have discussed above has been attributed to magnetic reconnection but this cannot be the mechanism at work in the Venus ionosphere. There is no magnetic field in the Venus ionosphere with which these ropes could interact. Here we believe that the shear in the flows in the Venus ionosphere simply rolls them up into twisted structures from initially straight strands of magnetic flux. The lesson here is that there may be more than one way to create similar magnetic structures. We should be careful not to attribute everything to the process known as magnetic reconnection.

4. Interaction of a Flowing Magnetised Plasma with a Magnetic Obstacle

From a distance the planetary magnetosphere appears to interact with the solar wind in much the same way that the planetary atmosphere and ionosphere interact as shown in Fig. 4. The magnetised plasma is deflected by the solar wind and because the flow is supersonic, a bow shock is formed that also heats and compresses the flow as it is deflected. However, the direction of the magnetic field of the planetary obstacle defines a reference direction for the interaction. When the solar wind magnetic field is parallel to the magnetic field at the ‘nose’ of the obstacle, the two fields become connected behind the polar cusp shown in Fig. 5. When the solar wind magnetic field is southward, the reconnection of the two fields occurs in the subsolar region (Dungey 1961). These two different sites of linkage lead to two quite different circulation patterns. Thus the interaction of the solar wind with the magnetosphere and the resultant circulation patterns change with variations in the direction of the interplanetary magnetic field. In turn, variations in the circulation of plasma lead to unsteadiness in the magnetosphere and give rise to the process known as the substorm, as illustrated in Fig. 15 (McPherron *et al.* 1973; Russell and McPherron 1973).

The changing states of reconnection at the magnetopause and in the tail current sheet certainly alter the force balance in the magnetosphere but they also produce flux ropes both at the magnetopause and in the tail. The flux rope at the magnetopause has been called a flux transfer event and the one in

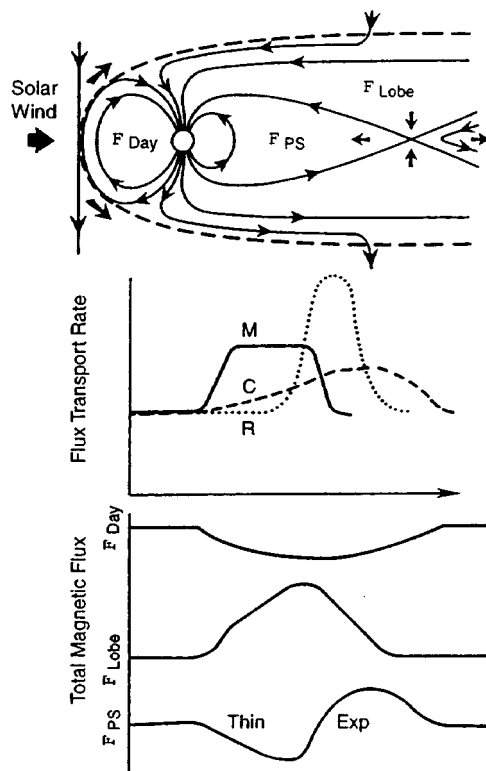


Fig. 15. Schematic illustration of the near-Earth neutral point model of the terrestrial substorm process. The top panel shows the magnetic configuration of the magnetosphere when the interplanetary magnetic field is southward. The substorm involves a change in the magnetic flux in the dayside magnetosphere F_{Day} , in the plasma sheet F_{PS} , and the tail lobes F_{Lobe} . The middle panel shows how the rate of transport between these three regions varies with time: M is the merging rate that converts dayside flux into tail lobe flux; R , the rate of reconnection in the tail that converts tail lobe flux to plasma sheet flux; and C , the rate of convection from the plasma sheet to the dayside magnetosphere. The bottom panel shows the amount of flux in each region when, after a period of northward interplanetary magnetic field, the field turns southward. The merging rate M responds immediately but the reconnection rate R in the tail does not increase until later, altering the relative amount of magnetic flux in each region. [After Russell (1994).]

the tail has been called a plasmoid. These structures very much resemble the structure of the ICME shown in Fig. 8. Here we can be certain that magnetic reconnection plays an important role in the production of the flux rope.

5. The Rapidly Rotating Magnetosphere

The jovian magnetosphere has long been known to be very active. As early as 1955, decametric radio emissions were discovered (Burke and Franklin 1955). Later, Bigg (1964) showed that Io controlled the occurrence of these emissions. It was soon speculated that Io was electrically conducting, enabling a current to flow through it powered by the potential drop associated with the rotating plasma in the magnetosphere (Piddington and Drake 1968; Goldreich and Lynden-Bell 1969). When the *Pioneer* and *Voyager* spacecraft arrived at Jupiter they found

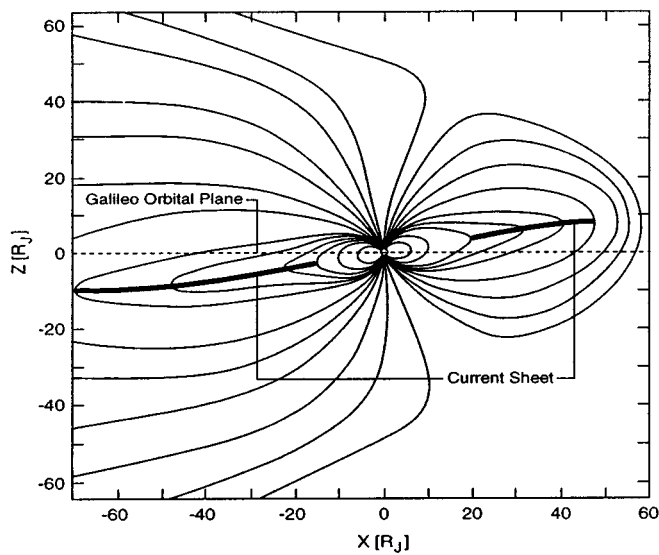


Fig. 16. Magnetic configuration of the jovian magnetosphere in the noon-midnight meridian (Russell *et al.* 1998). The centrifugal force of the ions added by Io at 6 jovian radii causes the magnetic field to become stretched into a magnetodisk configuration at all local times.

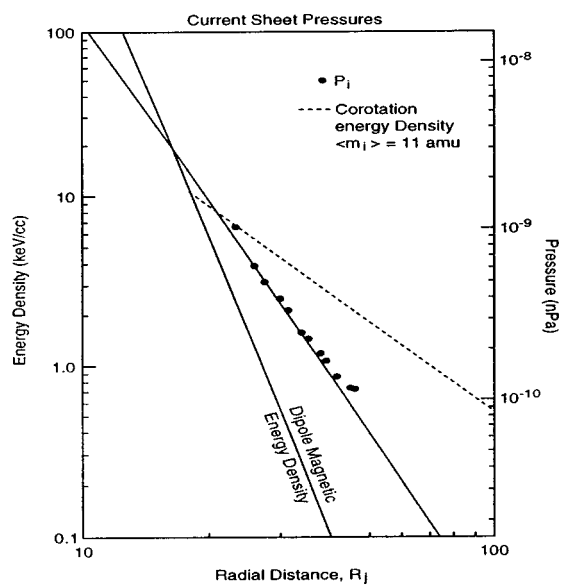


Fig. 17. Energy density and pressure of various constituents of the jovian magnetosphere as a function of radial distance: the magnetic energy of the dipole field, the particle pressure and the centrifugal force.

a rapidly rotating magnetosphere with a distended magnetodisk, as sketched in Fig. 16. The magnetodisk is caused by the addition of mass at Io, at up to 1 ton per second (Hill *et al.* 1983). Nevertheless the observation of a field-aligned current at Io reinforced the original interpretation that Io behaved as a unipolar inductor (Acuna *et al.* 1983).

The addition of a ton of heavy ions every second places a severe requirement on the radial transport of plasma in order to maintain a steady-state ion content in the magnetosphere. The observed density profile of the Io torus, the wake of Europa, the stress in the magnetodisk and the observed hot ion distribution all lead to a radial velocity profile that increases from about 9 m s^{-1} at $6.5 R_J$ to 50 km s^{-1} at $40 R_J$. Because the jovian magnetosphere rotates so rapidly (once in every 10 hours) and is so large, the centrifugal force is significant where it is not significant in other settings, such as in the terrestrial magnetosphere. Fig. 17 shows the various pressures estimated for the jovian magnetosphere. Inside about $16 R_J$ the dipole magnetic field dominates the pressure. From there to about $21 R_J$ the particle thermal pressure dominates and thereafter the centrifugal force, assuming the plasma is at full corotational velocity.

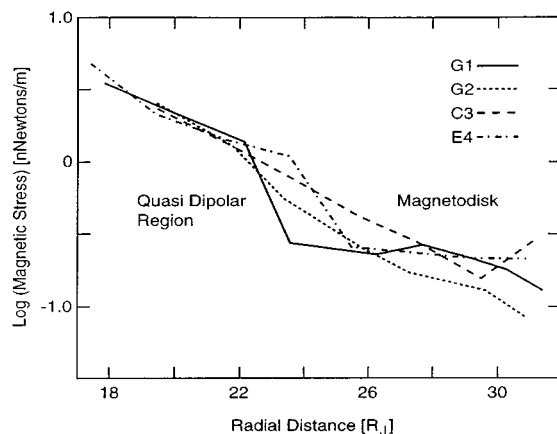


Fig. 18. Magnetic force calculated from the change in radial field across the current sheet and the field normal to the jovian current sheet, as a function of radial distance for the first four orbits of the *Galileo* mission. [After Russell *et al.* (1999).]

We know that the outgassing of Io is unsteady so we might expect that the density of the radial outflow would also be unsteady. We can check the constancy of the magnetodisk region by examining the magnetic force at each of the current sheet crossings. This calculation is made by using the changes in the radial magnetic field component across the magnetodisk as a measure of the current, and taking the cross product of that current with the normal component of the field crossing the magnetodisk. This magnetic stress is shown in Fig. 18 for the first four inbound passes (Russell *et al.* 1999). We see that inside about $22 R_J$ the stress is constant from orbit to orbit, but beyond $22 R_J$ it is variable. Sometimes the radial profile of stress is rather smooth. At other times it changes abruptly in the neighborhood of $24 R_J$. Clearly the properties

of the magnetodisk are variable but our analysis does not say what is changing. It could be the density, corotational velocity, plasma temperature etc.

The inner part of the magnetodisk current layer, from 24 to about 45 R_J , does not show evidence of tearing or reconnection of the oppositely directed magnetic fields bounding it. However, beyond 50 R_J in the local time sector midnight to 0300, the current sheet becomes very dynamic.

Fig. 19 shows one hour of magnetic observations in this region. The normal behaviour of the field would be a relatively constant field reversing its radial and azimuthal components as the current sheet was crossed. In contrast to expectation, there is a very strong transient in the direction normal to the current sheet that increases the field strength to a factor of three above the maximum pre-existing field strength.

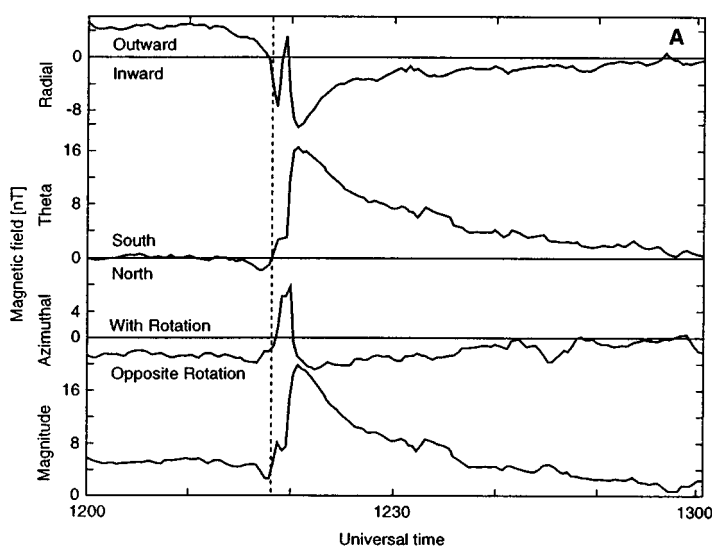


Fig. 19. Magnetic field in the near jovian tail during a substorm. The magnetic components are radially outward, southward and azimuthal in the corotation direction. The large increase in southward component indicates a strong reconnection event at greater radial distances. [After Russell *et al.* (1998).]

Not only has the reconnection event changed the direction of the field from horizontal to vertical, but it has increased the field magnitude. While reconnection events are seen in the Earth's tail current sheet, such large enhancements of the field strength do not occur. We attribute this enhancement to the presence of a highly rarefied plasma density in the regions above and below the current sheet, in which the Alfvén velocity is very high. Since the rate of reconnection is controlled by the Alfvén speed, when the reconnection region leaves the higher-density current sheet and reaches this rarefied plasma, the rate of reconnection increases rapidly and magnetic field piles up against the remaining inner current sheet. The geometry of the magnetic field after the onset of reconnection is shown in Fig. 20.

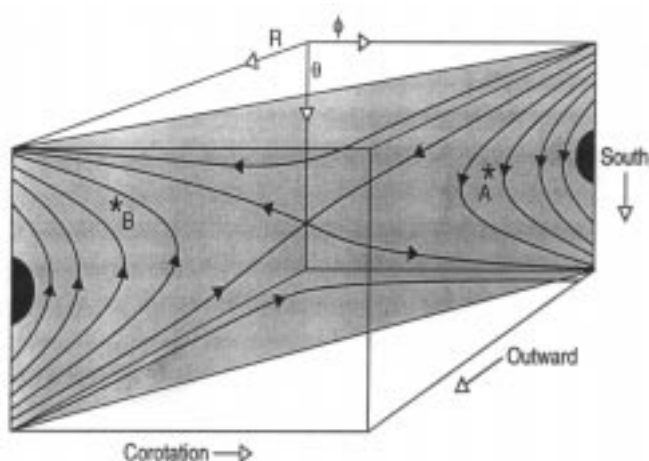


Fig. 20. Inferred magnetic field configuration in the near jovian tail during the reconnection event shown in Fig. 19 and during an event A when Galileo was at closer radial distances than the reconnection event. [After Russell *et al.* (1998).]

6. Summary and Conclusions

In this paper we have reviewed the forces in the magnetised plasmas of the solar system. These forces at times maintain an equilibrium in the plasma and at times take the plasma to a new equilibrium state. The magnetic force, the $\mathbf{j} \times \mathbf{B}$ force, can be separated into two components, a pressure gradient that acts perpendicular to the magnetic field and a force that acts toward the centre of curvature of the field line. Such forces can be self-balancing, such as a dipole field in a vacuum or in a force-free magnetic flux rope in a plasma with currents flowing only along the magnetic field. These forces can also be balanced by forces in the plasma such as pressure gradients, and centrifugal force. When plasma flows against an obstacle to the flow, the dynamic pressure or momentum flux of the flow enables one to calculate the force applied to the object by the flow.

Because of the high electrical conductivity of space plasmas, they tend to organise themselves into giant cells with roughly uniform properties, separated by thin current layers across which the properties change rapidly. When their directions are significantly different (e.g. antiparallel), the magnetic fields on opposite sides of the boundary may link up in the process known as reconnection. The new magnetic geometry created by the reconnection process can lead to plasma acceleration. If the accelerated plasma can expand into an essentially infinite reservoir, as, for example, the reconnected plasma at the nose of the magnetopause can do, then the reconnection process will in theory continue indefinitely. If the reconnected plasma is accelerated into a finite reservoir such as the night magnetosphere, then the process may shut itself off by causing the reconnection point to move away from the Earth. The energy for the accelerated plasma comes from the magnetic field. The coronal magnetic field, the Earth's magnetotail and the jovian magnetodisks can all store energy for later explosive release. Since the plasma is accelerated to the

Alfvén velocity, the magnetic field strength and the plasma density control the reconnection rate. When reconnection enters a region of very low density and high field strength, the rate of reconnection may increase rapidly, resulting in what has been termed explosive reconnection. Finally, magnetic flux ropes are being recognised throughout the solar system: in the corona, in the interplanetary medium, in planetary magnetopause current sheets and in magnetotail current sheets. These structures can be formed by magnetic reconnection or by velocity shears. They can vary in size from km to hundreds of millions of km in diameter. The importance of such structures is increasingly becoming appreciated. In particular, in the solar wind such structures are the most effective generators of geomagnetic activity because their twisted structure produces strong southward magnetic fields that interact with the Earth's northward field.

Acknowledgments

This work was supported by the National Aeronautics and Space Administration under research grants and through grants administered by the Johns Hopkins University Applied Physics Laboratory and the Jet Propulsion Laboratory.

References

- Acuna, M. H., Neubauer, F. M., and Ness, N. F. (1981). *J. Geophys. Res.* **86**, 8513.
- Bigg, E. K. (1964). *Nature* **203**, 1008.
- Burke, B. F., and Franklin, K. L. (1955). *J. Geophys. Res.* **60**, 213.
- Dungey, J. W. (1961). *Phys. Rev. Lett.* **6**, 47.
- Elphic, R. C., and Russell, C. T. (1983). *J. Geophys. Res.* **88**, 58.
- Goldreich, P., and Lyndell-Bell, D. (1969). *Astrophys. J.* **156**, 59.
- Hill, T. W., Dessler, A. J., and Goertz, C. K. (1983). 'Physics of the Jovian Magnetosphere', p. 353 (Cambridge Univ. Press: New York).
- Hundhausen, A. J. (1995). In 'Introduction to Space Physics' (Eds M. G. Kivelson and C. T. Russell), p. 91 (Cambridge Univ. Press: Cambridge).
- Lepping, R. P., Jones, J. A., and Burlaga, L. F. (1990). *J. Geophys. Res.* **95**, 11957.
- Luhmann, J. G. (1995). In 'Introduction to Space Physics' (Eds M. G. Kivelson and C. T. Russell), pp. 203–26 (Cambridge Univ. Press: Cambridge).
- McComas, D., *et al.* (1986). *J. Geophys. Res.* **91**, 7939.
- McPherron, R. L., Russell, C. T., and Aubry, M. P. (1973). *J. Geophys. Res.* **78**, 3131.
- Parker, E. N. (1979). 'Cosmical Magnetic Fields: Their Origin and Their Activity' (Clarendon: Oxford).
- Piddington, J. H., and Drake, J. F. (1968). *Nature* **217**, 935.
- Priest, E. R. (1995). In 'Introduction to Space Physics' (Eds M. G. Kivelson and C. T. Russell), pp. 58–90 (Cambridge Univ. Press: Cambridge).
- Russell, C. T. (1986). 'The Solar System Observations and Interpretations', pp. 311–58 (Prentice Hall: Englewood Cliffs, NJ).
- Russell, C. T. (1990). 'Physics of Magnetic Flux Ropes', pp. 413–23 (American Geophysical Union: Washington, DC).
- Russell, C. T. (1994). 'Strategies for the Tail and Substorm Campaign', pp. 24–31 (Boston University Center for Space Physics: Boston).
- Russell, C. T. (1995). In 'Introduction to Space Physics' (Eds M. G. Kivelson and C. T. Russell), pp. 1–26 (Cambridge Univ. Press: Cambridge).
- Russell, C. T., and Elphic, R. C. (1979). *Nature* **279**, 616.
- Russell, C. T., and McPherron, R. L. (1973). *Space Sci. Rev.* **15**, 205.
- Russell, C. T., *et al.* (1998). *Science* **280**, 1061.
- Russell, C. T., *et al.* (1999). *Planet Space Sci.*, **47**, 521.
- Saunders, M. A., and Russell, C. T. (1986). *J. Geophys. Res.* **91**, 5589.
- Walker, R. J., and Russell, C. T. (1995). In 'Introduction to Space Physics' (Eds M. G. Kivelson and C. T. Russell), pp. 164–82 (Cambridge Univ. Press: Cambridge).